京 都 大 学 防 災 研 究 所 年 報 第47号 C 平成16年3月
Annuals of Disas. Prev. Res. Inst., Kyoto Univ., No. 47 C, 2004

# Test on Collapse Behavior of 3D Full-Scale Steel Moment Frames Subjected to Cyclic Loading

Dawei LIU*, Tomohiro MATSUMIYA**,
Masayoshi NAKASHIMA,
Keiichiro SUITA

* COE Researcher, DPRI, Kyoto University
** Graduate Student, Graduate School of Engineering, Kyoto University

**Synopsis**

This paper reports on a full-scale test on a three-story, two-span by one-span steel moment frame to characterize the cyclic behavior beyond the deformation ranges considered in the contemporary seismic design. The following observations are noted: Balanced deformations between members were observed in contemporary deformation. In the larger deformation, pinching behavior was notable because of cyclic yielding at column bases, and composite action between steel beams and RC slabs decreased. The final failure occurred by first-story collapse mechanism promoted by severe deterioration of column bases. The effect of ALC panels on the structural behavior was nearly null.

**Keywords**: steel moment frame; full-scale test; seismic design; composite action; ALC panels; column base

## 1. Introduction

"Performance-based engineering" has become a standard norm for research, development, and practice of earthquake engineering particularly after the 1994 U.S. Northridge and 1995 Hyogoken-Nanbu (Kobe) earthquakes (Performance, 1995; Recommended, 2000; NEHRP, 2000; Notification, 2000; Midorikawa et al., 2003). Relevant themes of challenges range from the characterization of strong motions and their effects on the structural response, quantification of multiple levels of performance associated with the functionality, damage, and safety limit states, examinations into the interaction of various nonstructural components and building contents with building performance, among many others. To verify individual research findings and assure the expected performance of innovative developments and practices, real data obtained from "observations" and "experiments" are essential. They are rather difficult to acquire, however. A large earthquake event occurs very scarcely, which makes it difficult to monitor or measure the real behavior of structures at such an event. Interaction between member and system behavior is known to be complex; hence tests on a structural system that has

much redundancy are indispensable. Building structures, however, are massive, and it is difficult to fabricate and load them in the laboratory, whereas miniature models are known to fail to duplicate the prototype behavior because of lack of similitude. Considering these circumstances, the writers conducted an experimental project in which a full-scale, three-story steel building frame was loaded quasi-statically to failure. The primary objectives of the project were: (1) to acquire realistic data about performance, progress of damage, and final failure of the concerned frame in deformation ranges that are far beyond those considered in contemporary seismic design; (2) to examine the interaction between the local damage induced into individual members and elements and the global damage sustained by the structural frame; (3) to observe effects of RC floor slabs on the behavior of steel moment frames; and (4) to examine the interaction between the structural system and exterior finishes. This paper reports on the outline and preliminary results of this project in that the test was completed a few weeks before the time of this writing. First, the paper introduces the test structure and the adopted loading and measuring procedures. Second, the overall behavior of the test structure is outlined up to the deformation ranges approximately two to four times as large as those considered in the present Japanese seismic design. A beam fracture, its effect on the overall behavior, and the final failure mode were also noted. Third, composite action between the steel beam and RC floor slab and effects of exterior finishes (cladding) on structural behavior are discussed.

## 2. Test Structure

The test structure was a three-story, two-bay by one-bay steel moment frame as shown in Fig.1, having a plan dimension of 12 m (in the longitudinal direction) by 8.25 m (in the transverse direction). The structure was designed following the most common design considerations exercised in Japan for post-Kobe steel moment frames. That is, the columns were made of cold-formed square-tubes, beams were made of hot-rolled wide-flanges, the through-diaphragm connection details were adopted, in which short brackets were shop-welded to the columns [Fig.2(a)]. The columns with short brackets were transported to the test site, and they were connected horizontally to beams by high-strength bolts. Metal deck sheets were placed on top of beams, with studs welded to the beam top flanges through the metal deck sheets. Wire-meshes were placed above the metal deck sheets, and concrete was placed on site.

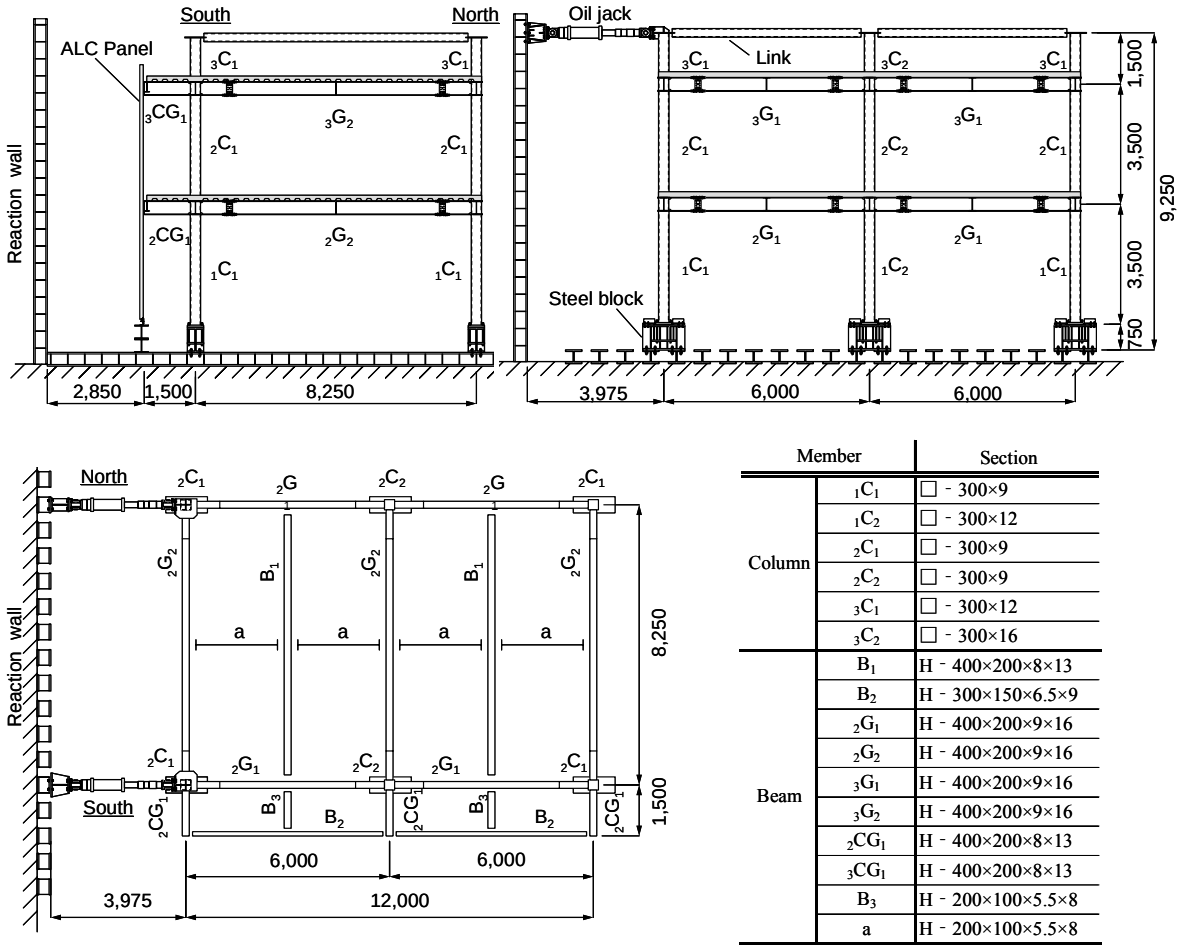


| Member | | Section |
|---|---|---|
| Column | $_1C_1$ | □ - 300×9 |
| | $_1C_2$ | □ - 300×12 |
| | $_2C_1$ | □ - 300×9 |
| | $_2C_2$ | □ - 300×9 |
| | $_3C_1$ | □ - 300×12 |
| | $_3C_2$ | □ - 300×16 |
| Beam | $B_1$ | H - 400×200×8×13 |
| | $B_2$ | H - 300×150×6.5×9 |
| | $_2G_1$ | H - 400×200×9×16 |
| | $_2G_2$ | H - 400×200×9×16 |
| | $_3G_1$ | H - 400×200×9×16 |
| | $_3G_2$ | H - 400×200×9×16 |
| | $_2CG_1$ | H - 400×200×8×13 |
| | $_3CG_1$ | H - 400×200×8×13 |
| | $B_3$ | H - 200×100×5.5×8 |
| | a | H - 200×100×5.5×8 |

Figure 1: Plan and Elevation of Test Structure (unit: mm)

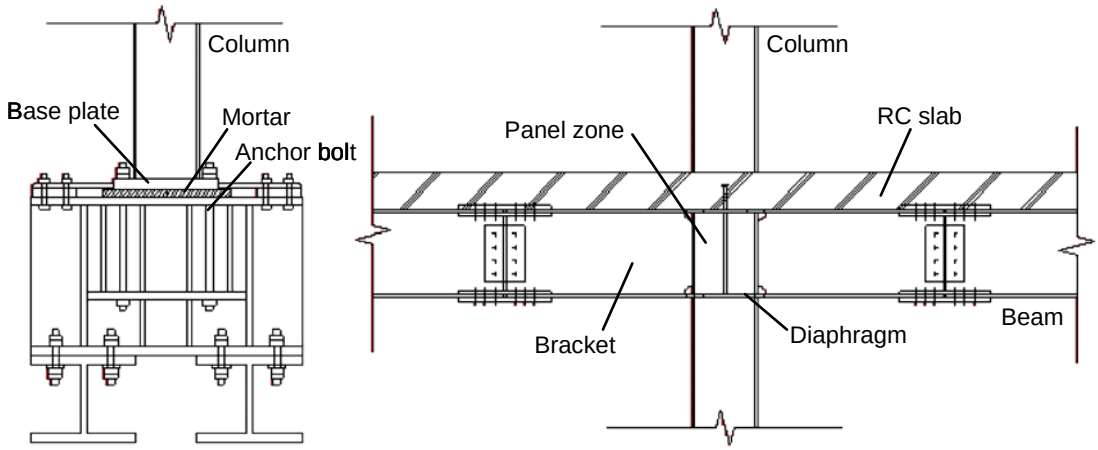


(a) Column Base Connection (b) Beam-to-Column Connection

Figure 2: Connection Details

Figure3: Overview of Test Structure (with ALC Panel)

Table 1: Material Properties of Steel and Concrete Used

| Sampled Plates | | Yeild strength (MPa) | Ultimate strength (MPa) |
|---|---|---|---|
| Column | □300×9,BCR295 | 386 | 456 |
| | □300×12,BCR295 | 393 | 459 |
| | □300×16,BCR295 | 399 | 451 |
| Beam | flange, SN400B | 287 | 434 |
| | web, SN400B | 347 | 455 |
| Diaphragm | PL-22, SN490C | 347 | 507 |
| Base plate | PL-50, SN490B | 315 | 461 |
| Ancor bolt | M33, SNR490B | 350 | 514 |
| | M36, SNR490B | 341 | 513 |
| Concrete | | 32.3 | |

Beam: H - 400×200×9×16

In the design of the test structure, yielding and plastic deformations were assigned for beam-ends, panel-zones, and column bases; hence the column-to-beam strength ratios ranged from 1.9 to 2.2. Fabrication and construction procedures adopted for the test structure faithfully followed those exercised in real practice (Nakashima et al., 1998). Exception was the column bases. Instead of embedding anchor bolts in the foundation RC beams, anchor bolts were fastened in short, deep steel beams, which in turn were securely tied down to the strong floor [Fig. 2(b)].

The two-planes placed in parallel in the longitudinal direction were nearly identical, but one plane, called the "South" plane, had a floor slab extended on the exterior side by 1.5 m, while the other plane, called the "North" plane, had a floor slab that terminated at the beam end (Fig.1). This overhang was designed to make it possible to directly measure the effects of RC floor slabs from the difference in resistance between the two planes. The columns were extended to the approximate mid-height in the third story, at which level steel braces were connected horizontally to the columns by high strength bolts through gusset plates. The braces served to achieve a rigid-diaphragm action in this plane, while the column rotations at the top were permitted by the out-of-plane flexibility of the gusset plates. Two quasi-static jacks, one in each longitudinal plane, were placed in this level, as shown in Fig.1.

Another feature of the test structure was the exterior finishes (cladding) installed during the test. ALC (autoclaved lightweight concrete) panels were placed on one edge of the floor to examine the effects of nonstructural elements on the hysteretic behavior of the test structure. The ALC panels were installed along the floor edge of the "South" plane (the one with the overhang) as shown in Fig.3.Material properties of the steel and concrete used for the test structure were obtained by tensile coupon and concrete cylinder tests. The properties thus obtained are listed in Table 1.

### 3. Loading Program

As shown in Fig.1, two quasi-static jacks were arranged for horizontal loading. They had a 3 MN force capacity and 800 mm stroke capacity. Each jack was placed at one end of the test structure and at the mid-height of the third story. An identical

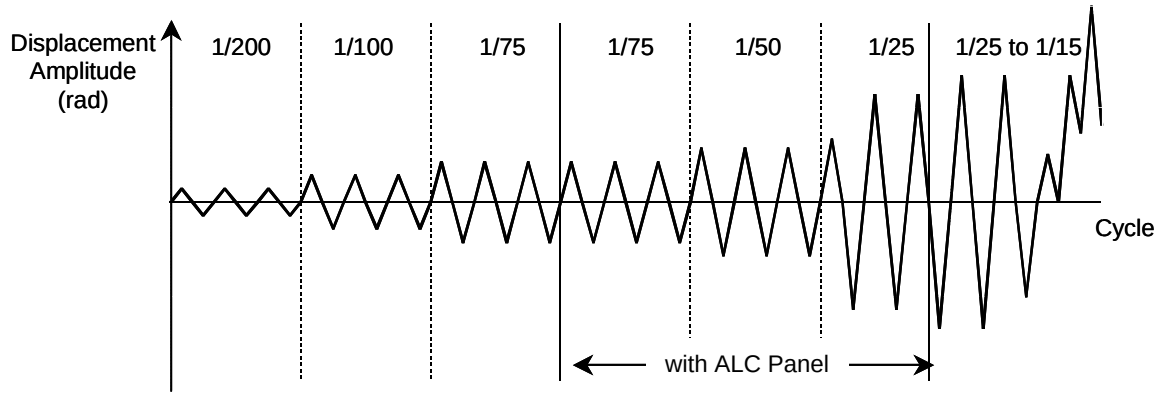


Figure 4: Loading Program

displacement was applied to both jacks. As explicated later, the two planes, taking the same displacement at the top, acted nearly independently; that is, no transfer of the force between the two planes was observed. This means that the load applied to each jack was the same as the force sustained by the concerned plane. Figure 4 shows the loading program used in the test. Quasi-static cyclic loading with increasing displacement amplitudes was adopted, and either two or three cycles were repeated for each amplitude. The displacement was expressed in terms of the overall drift angle, defined as the horizontal displacement at the loading point relative to the loading height (i.e., 8.5 m). Overall drift angles of 1/200 rad, 1/100 rad, 1/75 rad, 1/50 rad, 1/25 rad, and 1/20 rad were adopted. An on-line pseudo dynamic test was also conducted in the medium range of loading (after the 1/75 rad amplitude loading and before the 1/50 rad amplitude loading). After loading to the 1/20 rad amplitude, the jacks were dismounted once, and installed again with a 0.6 m long shim, and reloaded again to the maximum overall drift angle of 1/15 rad to examine the failure behavior.

A computer controlled on-line test system was used for the test. The system consisted of quasi-static jacks, load cells, digital displacement transducers, pump units equipped with inverter motors, controllers that controlled the pump units, a PC, called PC for Control, that supervised the controllers, and another PC, called PC for Operation, that was connected to PC for Control and commanded and sent displacement signals to PC for Control. PC for Operation was also connected on-line with a data logger having a scanning frequency of 1 kHz. The PC supervised the entire test operation to make loading and measurement fully automatic. The system was also capable of conducting the on-line pseudo dynamic test by running a program that solves the associated equations of motion in PC for Operation. The full detail of the control system is described in Nakashima et al., 1995 and Nakashima and Liu, 2003.

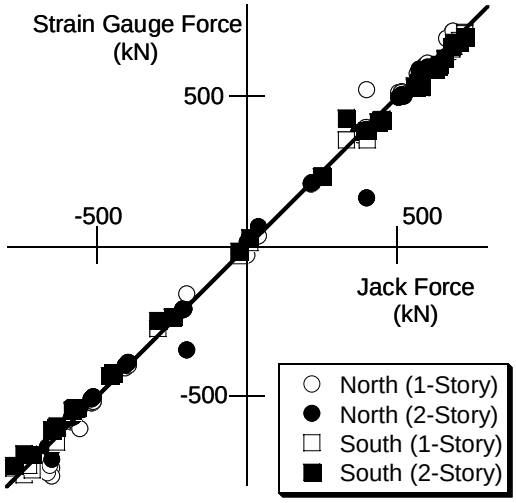


Figure 5: Comparison between Jack Force and Column Shear Estimated by Strain Gauge Reading

## 4. Measurement

A load cell attached to the head of each jack measured the horizontal load applied by the jack. A digital displacement transducer that had a resolution of 0.01 mm was used to measure the displacement of the jack. Four strain gauges were glued on the column surface at two cross-sections, each located at a distance of 1 m inward either from the column top or bottom. The cross-sections remained elastic; thus the bending moments applied at the cross-sections were estimated from the corresponding curvatures. The shear force applied to the column was estimated as the sum of the two bending moments divided by the distance between the measured cross-sections. According to the measured results, the shear force thus estimated was found very reasonable. Figure 5 shows comparison between the story shear measured by the jack's load cell (the horizontal axis) and the story shear estimated from the strain gauge reading (the vertical axis). They are plotted with respect to the story shear force at the peak drift angle (Fig.4) and with respect to the plane ("North" and "South") and

the story (first and second stories). All plots are located on and around the line inclined by 45 degrees of the horizontal axis, meaning that both story shears are very close to each other. The column axial force was estimated from the average of the strains measured by the column strain gauges. The beam shear force was estimated from the difference between the axial forces exerted into the two columns, one located on the top of and the other located underneath the concerned beam. Shear deformations of the panel zones, deformations of the floors in the direction orthogonal to the loading direction, rotations and lateral displacements of the column bases, and out-of-plane rotations and displacements of the beams were also measured by displacement transducers having a variety of gauge lengths. Furthermore, many strain gauges were glued on the beam flanges and webs in the vicinity of beam-to-column connections as well as on the anchor bolts at the column bases. These gauges were used to obtain information on local strains and deformations. Summing all the displacement transducers and strain gauges, a total of 283 data channels were connected to the data logger, which in turn was connected on-line to PC for Operation.

## 5. Test Result

### 5.1 Cyclic Loading Test

Figure 6 shows the relationship between the total force versus the overall drift angle, plotting the curves for loading from the amplitudes of 1/200 to 1/20 rad. Here, the total force was the sum of the loads applied by the two jacks. The solid monotonic line was an analytical curve obtained from pushover analysis, which was conducted in the course of designing the test structure. In the analysis, the effect of composite action between the wide-flange beam and RC floor slab was allowed for by multiplying the beam bending capacity by 1.5 times for positive bending (the bending in which the RC slab sustained tension). The analytically predicted initial elastic stiffness matched closely the experimental initial elastic stiffness, with the difference not greater than 8%. The analytical maximum strength was reasonably close to the experimental maximum strength, although the experimental strength revealed significant cyclic hardening (by about 30% beyond the yield strength). The results of Fig.6 suggest that nonlinear pushover analysis commonly used for seismic design practices is reasonable to predict the elastic stiffness and to estimate the maximum strength with some conservatism.

Figure 7 shows the story shear versus story displacement relationships. The relationships are presented with respect to the story (the first and second stories) and plane (the "North" and "South" planes). The story shear force was the load applied by the jack placed in the concerned plane. In the

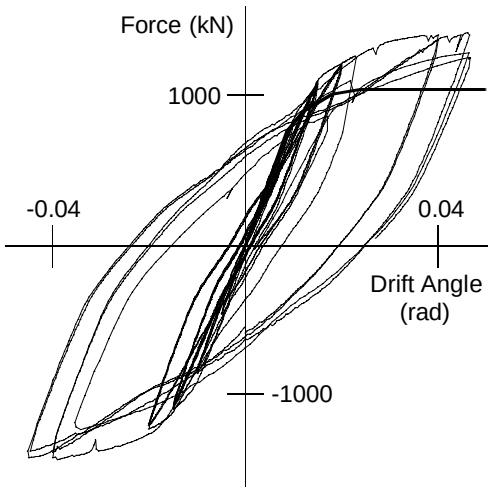


Figure 6: Total Load versus Overall Drift Angle Relationship

relationships shown in Fig.7, those obtained from the tests with ALC panels were excluded. For the loading not smaller than the 1/75 amplitude, beams, panel-zones, and column bases sustained plastic deformation, which indicates the balanced participation of individual components to the overall deformations. Pinching behavior in the second and third cycles relative to the first cycle was notable for the 1/75 amplitude and greater. This was primarily due to yielding and progress of plastic deformations of the anchor bolts. Such yielding was accepted in designing the test structure.

### 5.2 Fractures and Failure

Small but visible cracks started during the cycles of the 1/25 amplitude and grew either from the toe of the weld access hole or from the edge of the runoff tab at a few beam ends. These cracks had no visible effects on the global behavior as shown in Figs.6 and 7. During the first cycle in the positive loading of the 1/20 amplitude, the "North" plane's second floor beam was fractured from the beam bottom flange at the connection to the exterior column located on the loading jack's side (Fig.8). The fracture caused a sudden drop of the "North" plane's resistance by about 15% [Fig. 7(a)] but the incremental stiffness for the succeeding loading was positive again. Figure 9 shows the moment diagrams of the "North" plane just prior to the fracture of the beam flange [Fig. 9(a)] and right after the fracture [Fig. 9(b)]. The bending moments at member ends were estimated from the column shear and axial forces, as noted in Section: Measurement. The numbers inserted in the figure indicate the bending moment values at respective positions. A significant reduction in the bending moment is naturally observed at the fractured bean end, which also induced significant reduction in the bending moments at the first story's column top and second story's column bottom, both connected to the

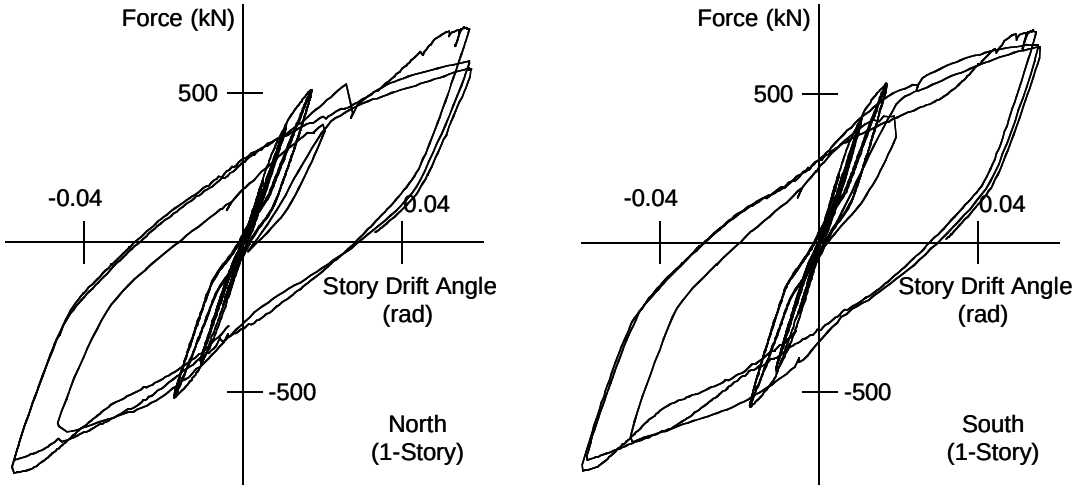


(a) First Story in "North" Plane (b) First Story in "South" Plane

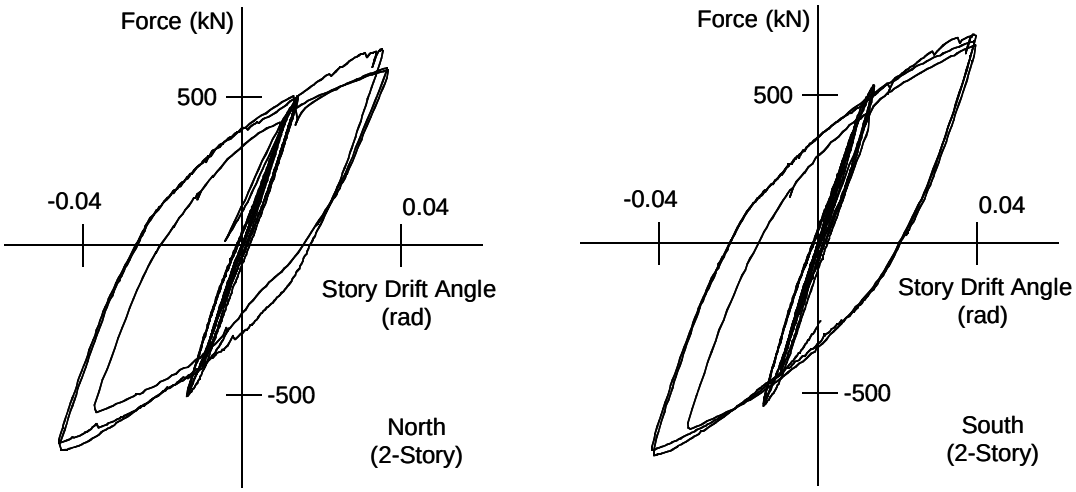


(c) Second Story in "North" Plane (d) Second Story in "South" Plane

Figure 7: Story Shear versus Story Drift Angle Relationships

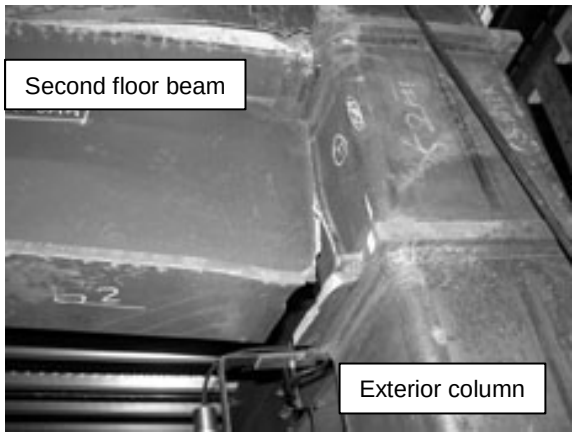


Figure 8: Fracture at Beam End

fractured beam end. It is notable that the bending moment values did not change much in all other locations. This indicates that effects of one fracture remain rather local, confined primarily in the vicinity of the fracture location. This observation is reasonable in light of the classical St. Venant's principle, as analytically explicated by Nakashima et al., 2000.

Figure 10 shows the story shear versus story drift angle relationship for the last portion of loading with large drift angles. The first story shear decreased significantly with the increase in story drift angle from 1/20 to 1/8 rad [Fig. 10(a)], whereas the second story was unloaded [Fig.10(b)]. Formation of a

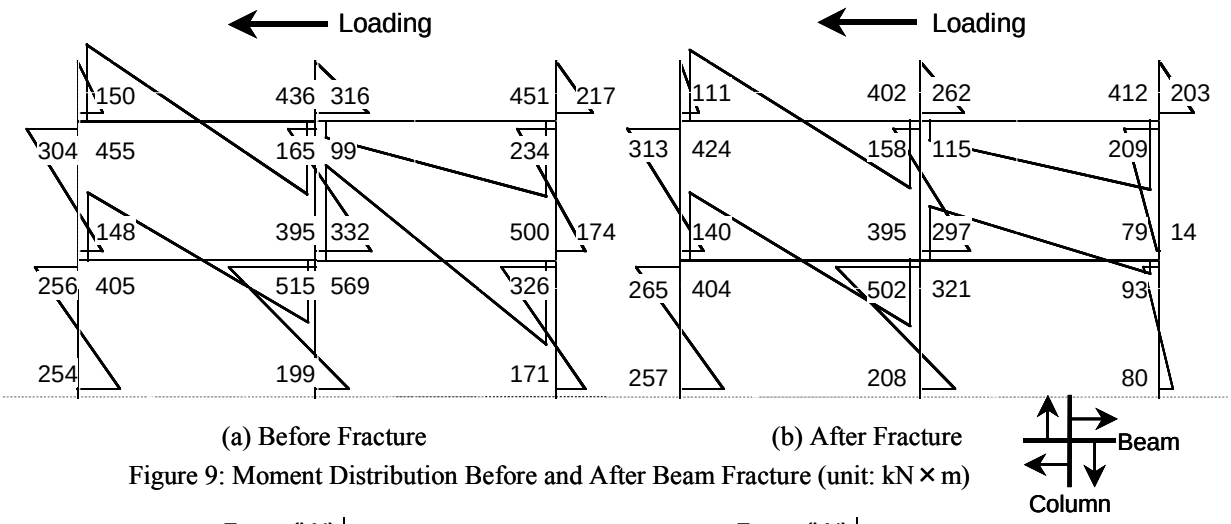


(a) Before Fracture (b) After Fracture

Figure 9: Moment Distribution Before and After Beam Fracture (unit: kN × m)

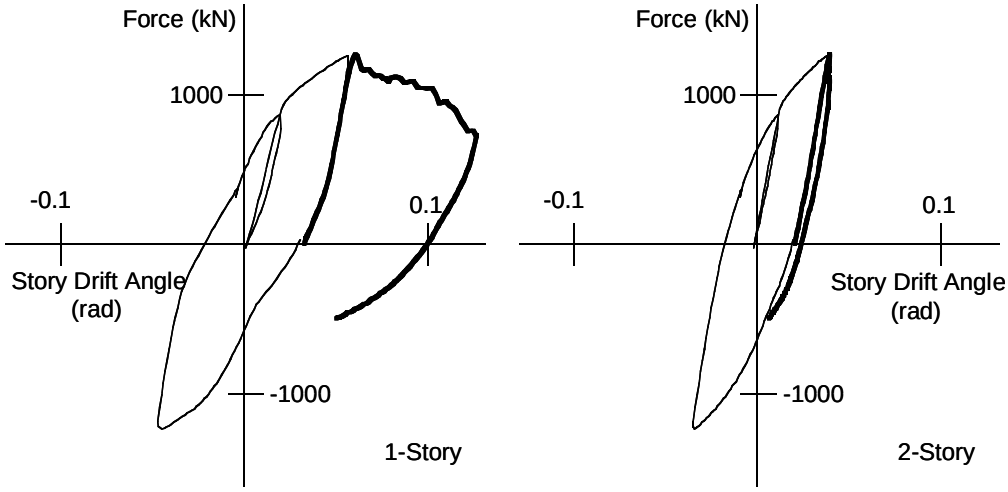


(a) First Story (b) Second Story

Figure 10: Unstable Behavior in Formation of First-Story Collapse Mechanism

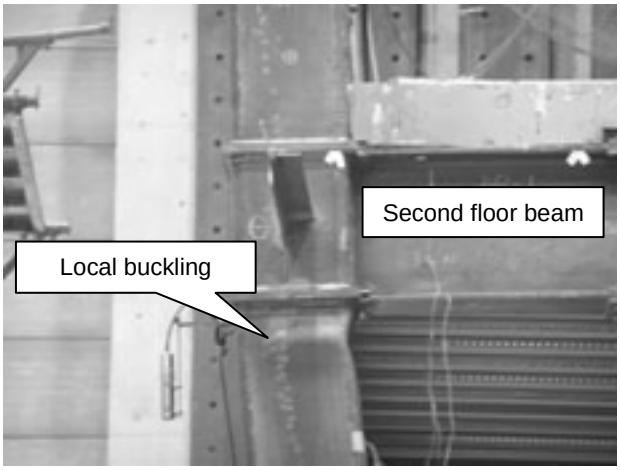


Figure 11: Local Buckling at First Story Column Top

first-story collapse mechanism was the primary reason for the drop in resistance. The moment resistance of the column bases decreased seriously during the last-stretch of loading, because of the combined effect of plastic elongation of anchor bolts and the crash of concrete placed underneath the column base plates. This decrease moved the column's inflection point lower and increased the bending moment at the column top, which eventually reached the plastic moment. The first story's unstable behavior was accelerated because of local buckling at the column top (Fig.11). The width-to-thickness ratios of the first story columns were 25 (interior columns) and 33 (exterior columns), which

were not compact in the classification of AISC 2000 Seismic Provisions.

### 5.3 Composite Actions

Figure 12 shows the crack patterns observed up to the overall drift angle of 1/25. The three lines of cracks running horizontally (from "North" plane to "South" plane) were the shrinkage cracks present prior to loading. These cracks ran on top of the orthogonal beams where shear studs were arranged. To the overall drift angle of 1/25, cracks were accumulated along the longitudinal beams and extended approximately 1 m on both side of the beam. Although preliminary, the effect of composite action was estimated as follows. The difference in stiffness and strength between the "South" and "North" planes was taken to be half the composite effect in that the "South" plane had the floor slab on both sides of the beam, whereas the "North" plane had the floor slab only on one side. Thus, the "North" plane's strength (or stiffness) minus the difference of strength (or stiffness) between the two planes was taken to be the strength (or stiffness) of the bare steel frame (without the RC floor slabs), and twice the difference was taken to be the increase by the composite action. Table 2 summarizes the increase of strength and stiffness by the composite action thus estimated. Composite action led the test structure to an increase of the elastic stiffness (during the 1/200 rad amplitude) by about 30%. The action became less notable with the increase in amplitude most likely because of cracks accumulated in floor slabs. Under the 1/25 rad amplitude, the effect was reduced to 5%.

### 5.4 Interaction with Exterior Finishes

The effects of exterior finishes on the stiffness and strength of the tested frame were observed by the direct comparison between the tests with the 1/75 and 1/25 amplitudes, because for those two amplitudes, tests were conducted one time without the ALC panels and the other time with them. The panels were attached to the edge beam of the "South" plane. Configuration of the ALC panels and the attachment details are shown in Fig.13. The ALC panels had a width of 600 mm, a height of either 3,500 mm (the first story) or 3,960 mm (the second story) mm, and a

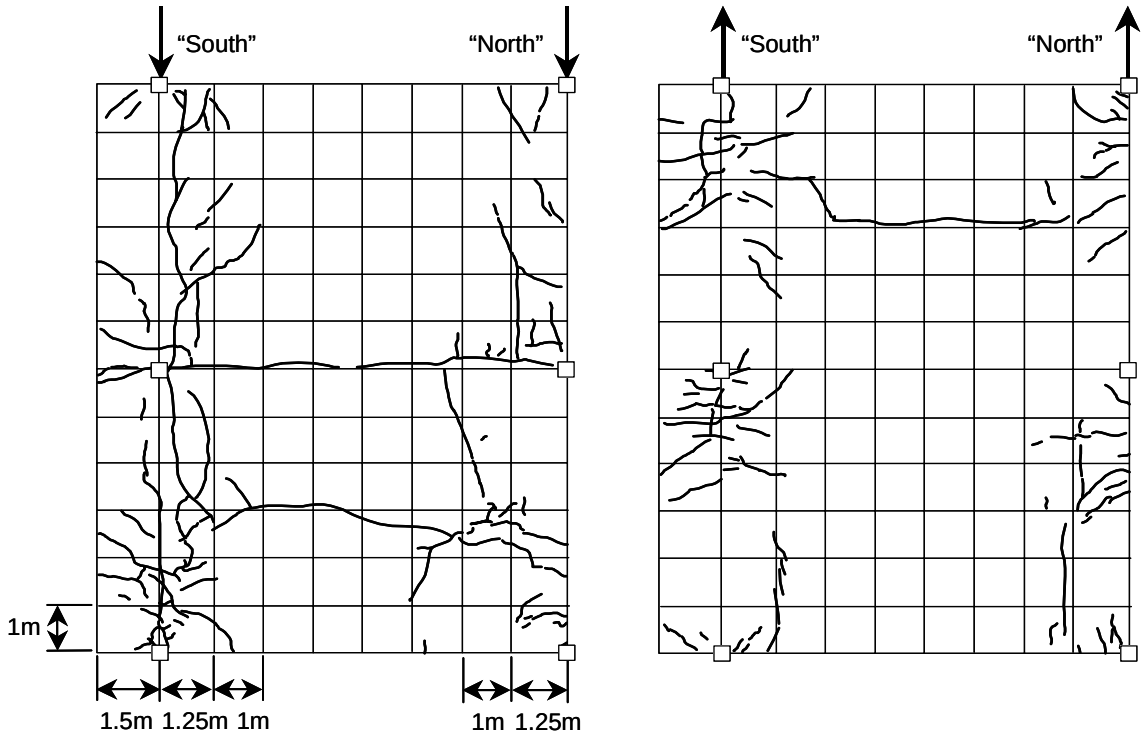


(a) Positive Loading (b) Negative Loading

Figure 12: Cracks Formed During Loading

Table 2: Summary of Composite Action With Respect to Cyclic Amplitude

| | Bare frame | Composite effects | Total | Percentage in increase |
|---|---|---|---|---|
| Initial stiffness (kN/mm) | 4.3 | 1.2 | 5.5 | 28% |
| 1/200 (kN) | 183 | 50 | 233 | 27% |
| 1/100 (kN) | 369 | 52 | 421 | 14% |
| 1/75 (kN) | 489 | 44 | 533 | 9% |
| 1/25 (kN) | 571 | 30 | 601 | 5% |

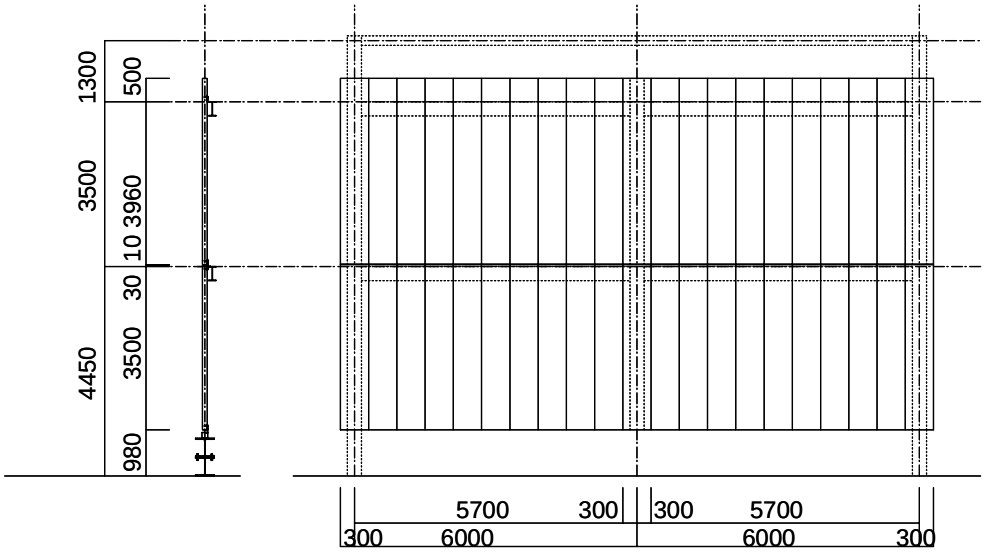


(a) Elevation

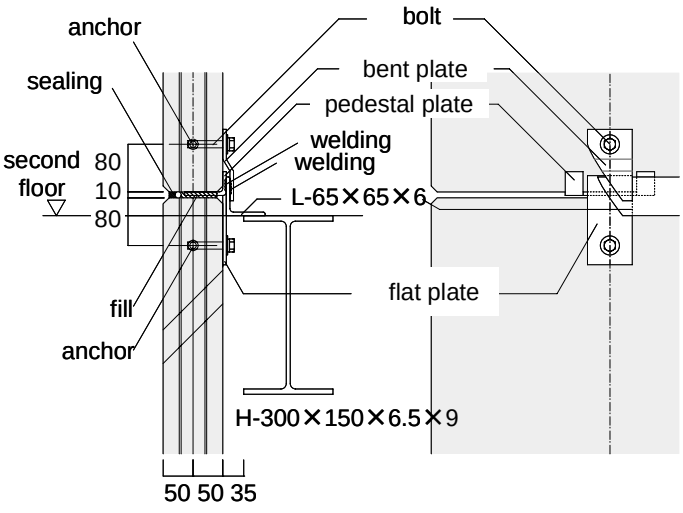


(b) Attachment to Edge Beam

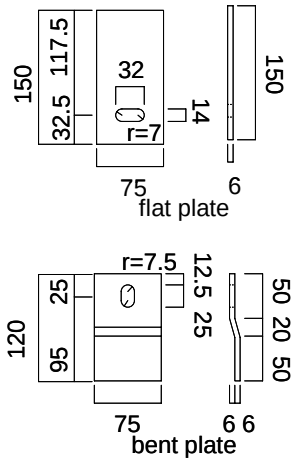


(c) Plates with Slotted Holes

Figure 13: Installation of ALC Panels

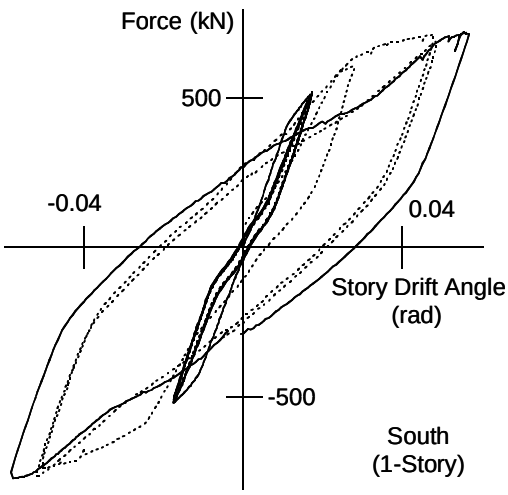


(a) First Story

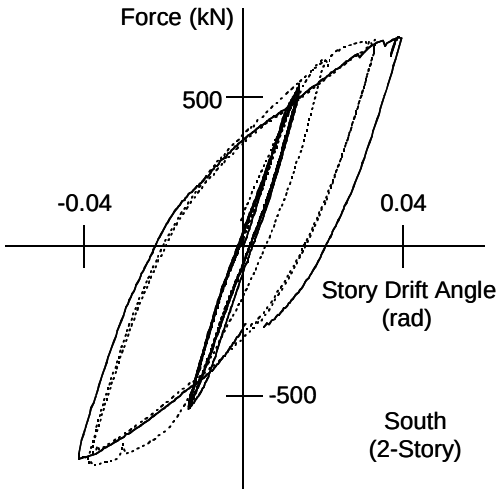


(b) Second Story

Figure 14: Effect of ALC Panels on Hysteretic Behavior
(Solid Lines = without Panels; Dotted Lines = with Panels)

(a) Inclination of ALC Panels (1/25 rad Drift)

(b) Cracks and Spalling of Concrete at Panel Bottom

Figure 15: Deformation of ALC Panels

thickness of 100 mm [Fig. 13(a)]. Each panel had a stud bolt embedded in the mid-width location near the top and bottom edge. The bolt was inserted to the slotted hole of a small steel plate [Fig.13(c)]. The plate was welded to a small angle, and the angle was welded to the edge beam [Fig. 13(b)], both prior to the installation of the ALC panels. The slotted holes were used to ensure rigid movement of the ALC panels during the horizontal response of the frame. This detail has been adopted widely in Japan particularly after the 1995 Kobe earthquake, in which quite a few damage instances were observed for ALC panels (Reconnaissance 1995).

Figure 14 shows the "South" plane's story shear versus story drift relationships obtained for the two amplitudes, with the solid lines without the ALC panels and the broken lines with. As evidenced from the figures, the ALC panels did not affect either the stiffness or strength for both amplitudes. Product specifications of ALC panels commonly specify an allowable story drift of 1/75 to 1/50 for use in practice. The test results showed excellent performance of the ALC panels and adequacy of the attachment details [Fig. 13(b) and (c)]. No visible cracks were observed in the ALC panels except for minor cracks and spalling of concrete at the bottom of the panels in the first story (Fig.15). At this location, there were inevitable contacts between the panels and the pedestal angle when the panels rotated.

## 6. Conclusions

This paper introduced the outline and preliminary results of the cyclic loading tests applied to a full-scale, three-story, two-bay by one-bay steel moment frame. Although detailed data processing, interpretation of the results, and post-analyses are still in progress, the writers obtained the following notable observations.

(1) Balanced deformations between the beams, panel-zones, and column bases (primarily due to yielding of the anchor bolts) were observed. Pinching behavior was notable for cyclic loading with larger amplitudes (up to 1/25 in the overall drift angle) primarily because of cyclic yielding and resulting slip-type hysterisis experienced at the column bases.

(2) A beam fracture caused changes in the bending moment distribution, but the effects were confined primarily in the vicinity of the fractured beam. This observation was consistent with the classical St. Venant's principle.

(3) Although the column-to-beam strength ratio was not smaller than 1.9, the final failure occurred by the formation of a first-story collapse mechanism. The mechanism was formed as a result of significant reduction in strength and stiffness of the column bases under large rotations and accelerated by local buckling of the column tops in the first story.

(4) The degree of composite action changed in accordance with the deformation amplitude; increases in strength became less notable (meaning that the composite effect decreased) for larger deformation amplitudes. This observation was understandable in reference to the accumulation of concrete cracks during cyclic loading with increasing amplitudes.

(5) The effect of ALC panels (used for exterior finishes) on the structural behavior was nearly null up to the story drift angle of 1/25 rad, indicating that the attachment details adopted for installation of ALC panels were very satisfactory in terms of the detachment of the panels from the frame response.

**Acknowledgements**

This research was supported by the Japanese Ministry of Education, Culture, Sports, Science and Technology (MEXT) 21st Century COE Program for DPRI, Kyoto University (No.14219301, Program Leader: Prof. Yoshiaki Kawata). The test presented in the paper was also part of a research projected entitled "Development of reliability seismic design in consideration of uncertainties associated with both

demand and capacity of structural systems." The third writer was the principal investigator of this project, and it was sponsored by the Ministry of Education, Culture, Sports, Science and Technology (Basic Research Category S: 14102028). The writers express their gratitude for the sponsorship. The writers are also grateful to Prof. K. Inoue of Kyoto University and Messrs. Y. Fujita and T. Arai of Obayashi Corporation for their continuous support on the design, construction, instrumentation, and loading of the test structure.

## References

Midorikawa, M., Okawa, I., Iiba, M., and Teshigawara, M. (2003), "Performance-Based Seismic Design Code in Japan", *Earthquake Engineering and Engineering Seismology*, Taiwan, Vol.4, No. 1 (pp. 12−25).

Nakashima, M., Akazawa, T., and Igarashi, H. (1995), "Pseudo Dynamic Testing Using Conventional Testing Devices", *Journal of Earthquake Engineering and Structural Dynamics*, Vol.24, No.10 (pp. 1409-1422).

Nakashima, M., Inoue, K., and Tada, M. (1998), "Classification of Damage to Steel Buildings Observed in the 1995 Hyogoken-Nanbu Earthquake", *Engineering Structures*, Vol.20, No.4-6 (pp. 271-281).

Nakashima, M., and Liu, D. (2003), "Instability and Complete Failure of Steel Columns Subjected to Cyclic Loading", *Journal of Engineering Mechanics, ASCE*, (submitted for publication).

Nakashima, M., Minami, T., and Mitani, I. (2000), "Moment Redistribution Caused by Beam Fracture in Steel Moment Frames", *Journal of Structural Engineering*, ASCE, Vol.126, No.1, January 2000 (pp. 137-144).

*NEHRP Recommended Provisions for Seismic Regulations for New Buildings and Structures.* (2000), FEM368, Federal Emergency Management Agency, Building Seismic Safety Council, Washington, D.C.

*Notification No.1457-2000, Technical Standard for Structural Calculation of Response and Limit Strength of Buildings.* (2000), Ministry of Land, Infrastructure and Transport (in Japanese).

*Performance-Based Seismic Engineering of Buildings.* (1995), SEAOC Vision 2000 Committee, Structural Engineers Association of California, Sacramento CA.

*Recommended Seismic Design Criteria for New Steel Moment-Frame Buildings.* (2000), FEMA350, Federal Emergency Management Agency, Building Seismic Safety Council, Washington, D.C.

*Reconnaissance Report on Damage to Steel Building Structures Observed from the 1995 Hyogokken-Nanbu Earthquake*. (1995), Steel Committee of the Kinki Branch of the Architectural Institute of Japan, Osaka.

## 要　旨

鋼構造物の耐震能力を定量化するため，3層実大鋼構造骨組を対象に，それが耐力を失うまでの挙動を実験的に検証した．耐震設計で考えられる変形領域までは，骨組各部材はバランスよく変形した．しかし，より大きな変形領域では柱脚部の降伏によるピンチング効果が現れ，さらに床スラブと梁の合成効果が低減した．最後に柱脚損傷の蓄積が柱降伏型の1層崩壊を誘発した．ALC版が構造挙動に及ぼす影響は無視できる．

**キーワード**: 鋼構造骨組; 実大実験; 耐震設計; 合成効果; ALCパネル; 柱脚